Supplementary Material for:

Metabolic physiology explains macroevolutionary trends in the melanic colour system across amniotes

Chad M. Eliason and Julia A. Clarke

Table of contents:

Supplementary Methods

***Assessing taxon sampling*–In total, we obtained morphological data for 255 species in the final tree (see figure S1). To assess the evenness of this taxonomic sampling, we used mean nearest taxonomic distance (MNTD) [1]. We calculated the MNTD for species with morphological data and compared this value to a null distribution generated by randomly shuffling tips [1]. The observed MNTD was ~58 My, which was not significantly smaller than expected by chance (P_{rand} = 0.13) suggesting that our sampling is not significantly biased or uneven [1].**

***Incorporating fossils*–We added extinct lepidosaurs and turtles with available melanosome data either as polytomies at the base of the Iguanidae clade or as the sister taxon to the lone extant representative of the Testudines clade, respectively, following [2]. For theropod dinosaurs, we used the R code, fossil ages, and published cladogram of [3] to generate a fossil subtree with the timePaleoPhy function in paleotree [4]. We grafted this time-calibrated fossil tree along the branch leading to birds in our extant supertree using custom R code (available on Dryad). Additional extinct archosaur taxa not represented in the published theropod tree [3] were added as sister taxa to clades in the supertree based on published divergence times [3,5] and with fossils as minimum ages [2]. Finally, we added three additional fossil taxa as polytomies (1 undescribed pterosaur, 1 undescribed psittaocosaur, and 1 undescribed enantiornithine; see table S1 for specimen details).**

***Sensitivity analysis*–Comparative methods that estimate shifts in the rate of phenotypic evolution generally do not require a fully resolved phylogeny, but rather that taxa are sampled uniformly with respect to the trait of interest [6]. To assess the sensitivity of our rate analyses to taxon sampling, we employed a jackknife approach following [7]. To do this, we created 25 subtrees by randomly removing 10 taxa. We then re-ran rate shift analyses on all random subtrees. The results show that the inferred rate shifts in Maniraptora (dinosaurs and birds) and Passeres (songbirds) are robust to removal of taxa (n=10), while the decrease in evolutionary rate at the base of the Sauropsida clade (non-avian reptiles, birds, crocodiles) is not (figure S3). This could be because of denser sampling of taxa with fossil melanosomes in feathered dinosaurs and birds (figure S2).**

***Clade-specific trends in evolutionary rates*– We compared among clade differences in evolutionary rates and covariation among traits using a Bayesian approach implemented in the ratematrix package [8]. This method reconstructs shifts in evolutionary trait correlations and rates while accounting for uncertainty in when different integumentary structures evolved. We used stochastic character mapping [9] to map integument type (hair, skin/scales, and feathers) onto the pruned phylogeny, with the ancestral state of integument type to skin/scales based on extant and fossil evidence [10]. We fit separate models for brown and black colours for melanosome length and melanosome diameter. We ran two MCMC chains for 2 million generations each and assessed convergence (Gelman-Rubin $R < 1.01$) with the checkConvergence function [8]. We compared evolutionary rates and covariation among**

clades by calculating posterior distribution overlaps in the testRatematrix function [8].
Overlaps >5% suggest that clades do not show distinct macroevolutionary trends.

SUPPLEMENTARY TABLES

Table S1. List of fossil taxa used. Data for samples 1-18 taken from Li et al. 2014 [2] and images used to measure melanosomes in sample 19 taken from McNamara et al. 2009 [11].

Sample	Taxon	Catalogue number
1	*Anchiornis huxleyi*	BMNHC PH828
2	*Archaeopteryx lithographica*	MB.Av.100
3	*Caudipteryx zoui*	PMOL AD00020
4	*Confuciusornis sanctus*	CUGB G20070001
5	*Inkayacu paracasensis*	MUSM 1444
6	Undescribed ornithurine	CUGB G20100053
7	*Microraptor*	BMNHC PH881
8	Undescribed enantiornithine	CUGB P1201
9	Undescribed enantiornithine	CUGB G20120001
10	*Beipiaosaurus*	BMNHC PH000911
11	*Sinosauropteryx*	IVPP V14202
12	Undescribed pterosaur	BMNHC PH000988
13	Undescribed pterosaur	PMOL AP00022
14	*Psittacosaurus lujiatunensis*	PKUP V1050
15	*Psittacosaurus lujiatunensis*	PKUP V1051
16	Undescribed turtle	PKUP V1070
17	*Xianglong zhaoi*	PMOL 000666
18	*Yabeinosaurus sp.*	PKUP V1059
19	Undescribed frog	MNCN 63805

Table S2. Relationship between rates of melanosome shape evolution and predicted metabolic rates in amniotes. Results of 'rate-by-state' tests. P values < 0.05 indicate rates of melanosome shape evolution are significantly correlated with predicted ancestral metabolic rates for black (eumelanin-consistent) colours, brown (phaeomelanin-consistent) colours, and species mean values ("All"). Significance was assessed by simulating trait evolution 500 times.

Colour	r	P value
Black	0.270	0.004
Brown	0.303	0.010
All	0.189	0.006

Table S3. Bayesian phylogenetic mixed models (BPMM) results. Columns show response variables and estimates with 95% Bayesian credible intervals calculated with the HPDinterval function in coda [12]. For multivariate response models, Wald tests showed overall significance between melanosome morphology and metabolic rate for black **(eumelanin-consistent)** colours ($p < 0.001$) but not brown **(phaeomelanin-consistent)** colours ($p = 0.52$).

Response	Term	Estimate (95% CI)	P_{MCMC}
Univariate	Intercept	2.36 (2.07, 2.65)	< 0.001
(aspect ratio)	Colour (brown)	-0.46 (-0.86, -0.10)	< 0.001
	BMR	0.65 (0.30, 1.04)	0.019
	BMR:Colour (brown)	-1.00 (-1.48, -0.51)	< 0.001
Multivariate	Length	6.63 (6.54, 6.73)	< 0.001
(length, diameter)	Diameter	5.85 (5.75, 5.95)	< 0.001
	Length:BMR	0.36 (0.24, 0.48)	< 0.001
	Diameter:BMR	0.15 (0.02, 0.29)	0.027
	Length:Colour (brown)	-0.27 (-0.41, -0.13)	< 0.001
	Diameter:Colour (brown)	-0.07 (-0.20, 0.07)	0.33
	Length:BMR:Colour (brown)	-0.44 (-0.62, -0.24)	< 0.001
	Diameter:BMR:Colour (brown)	-0.13 (-0.31, 0.05)	0.16

Table S4. Quadratic discriminant function analysis performance with and without including body mass. Variables included: melanosome length, melanosome diameter, melanosome aspect ratio, and log mass (for 'Mass' model only). See [13] for details.

Model	Cross-validation	Self-test
No mass	0.753	0.630
Mass	0.798	0.686

SUPPLEMENTARY FIGURES

Figure S1. Full synthetic supertree and taxon sampling in amniotes. Tips coloured according to clade (red: birds, blue: mammals, green: non-avian reptiles), with darker shades indicating species with morphological data (n = 255) and lighter shades without morphological data. Species without morphological data were dropped from the tree prior to analysis. A tree file with readable tips is available on Dryad.

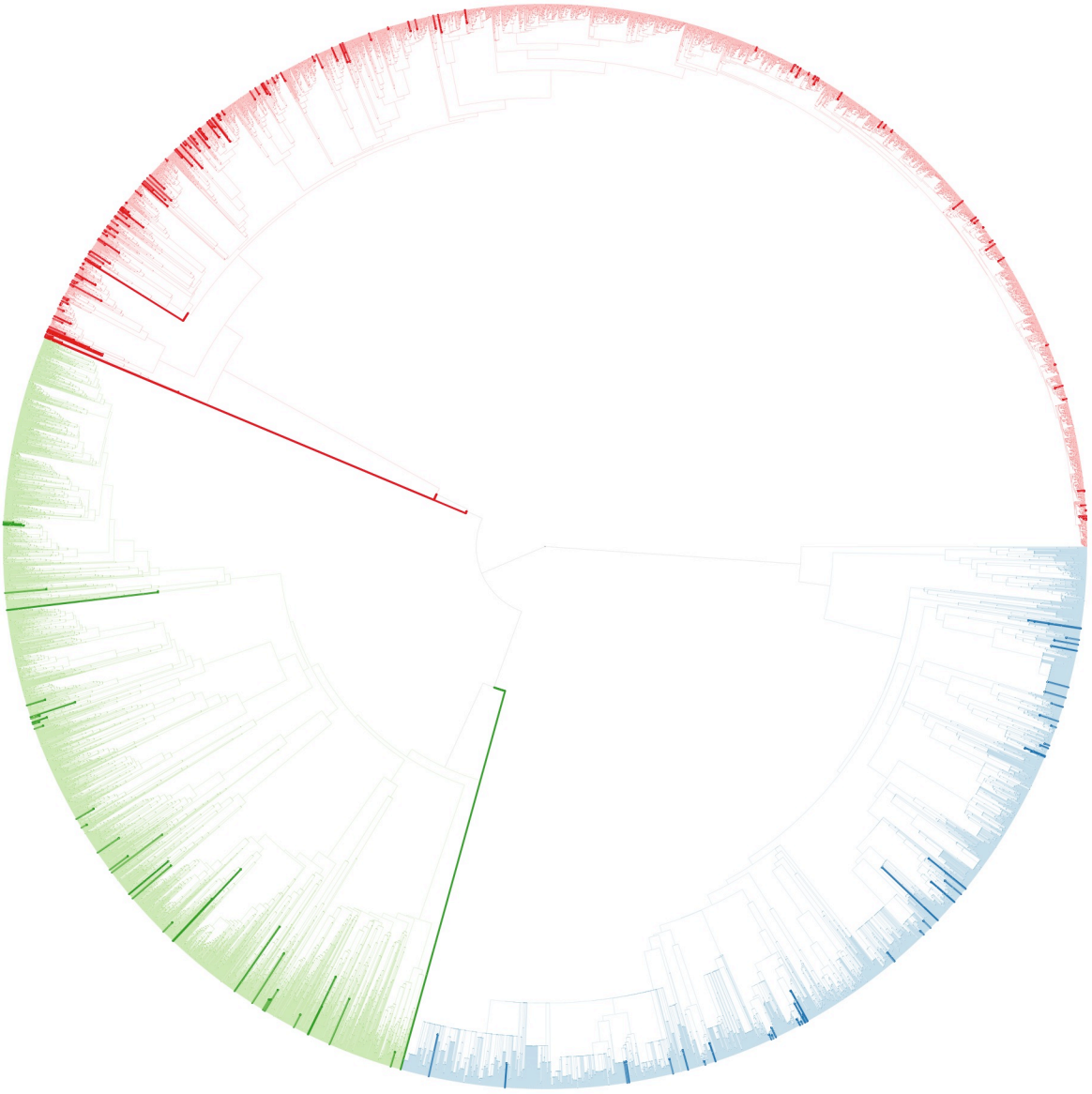

Figure S2. Full auteur rate shift results. Branch colours correspond to estimated rates of melanosome evolution (blue: slow, red: fast). Circles at nodes indicate estimated locations of rate shifts, with size of circle indicating probability of a rate shift occurring at a given node.

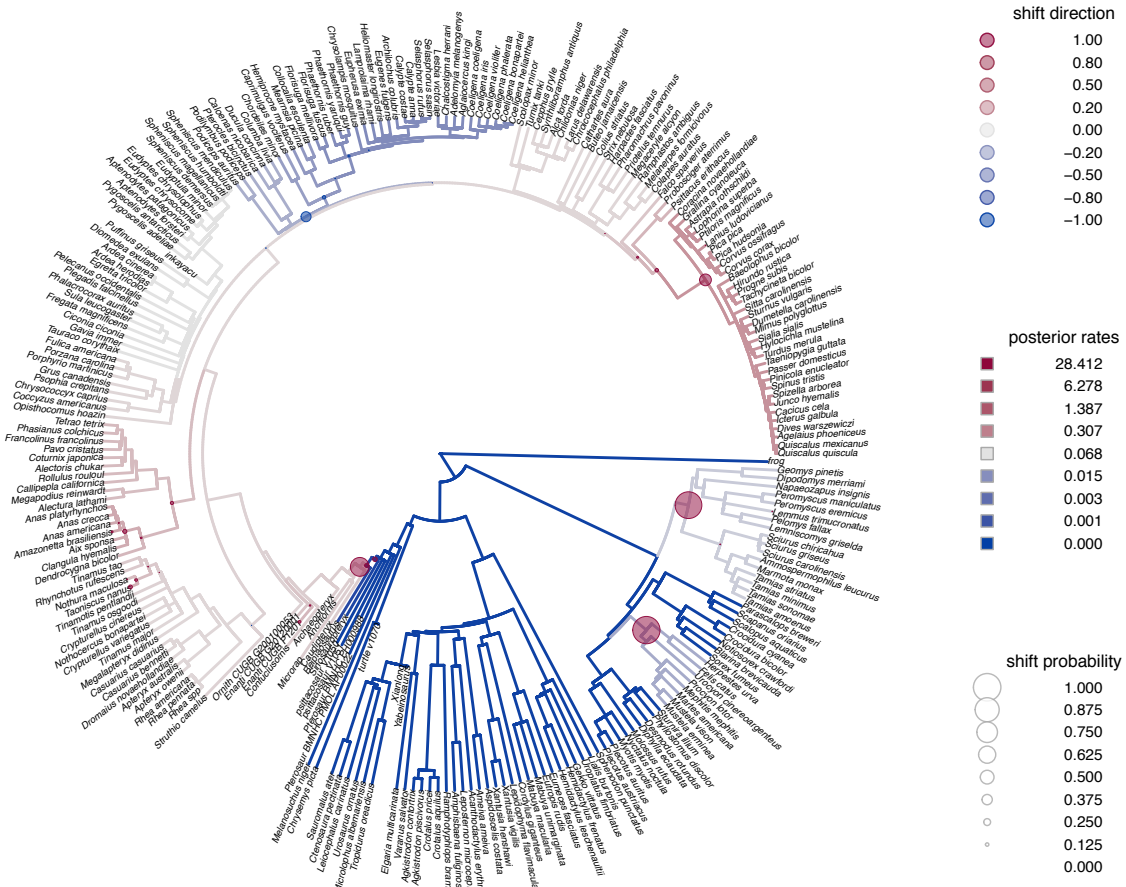

Figure S3. Sensitivity analysis for rate shifts estimated with auteur. Points show estimated shift probabilities for clades of interest (nodes highlighted in figure S2) after randomly removing 10 taxa from the tree (i.e. 'taxonomic jack-knifing'). This analysis indicates the shifts in Maniraptora (feathered dinosaurs and birds) and Passeres (songbirds) are robust to taxon removal, but the decrease in evolutionary rate at the base of the Sauropsida clade (non-avian reptiles, birds, crocodiles) is not. Values prior to jack-knifing are shown in blue.

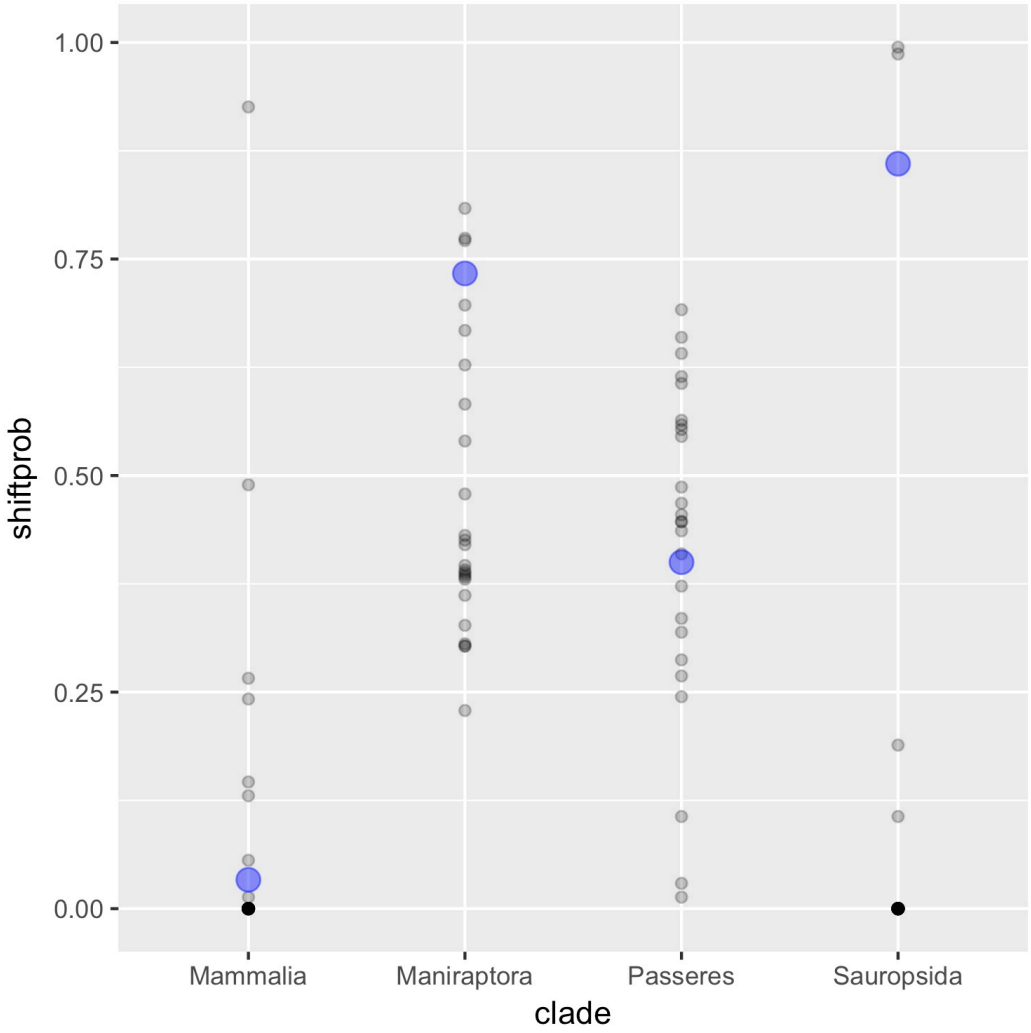

Figure S4. Clade-specific differences in rates of melanosome shape evolution for black (eumelanin-consistent) integument colours. Plots show posterior distribution of evolutionary rates (plot diagonals) and covariation (off-diagonal plots) between melanosome length and diameter for birds (red), mammals (blue), and non-avian reptiles (green). Birds and mammals show higher rates of morphological evolution compared to non-avian reptiles.

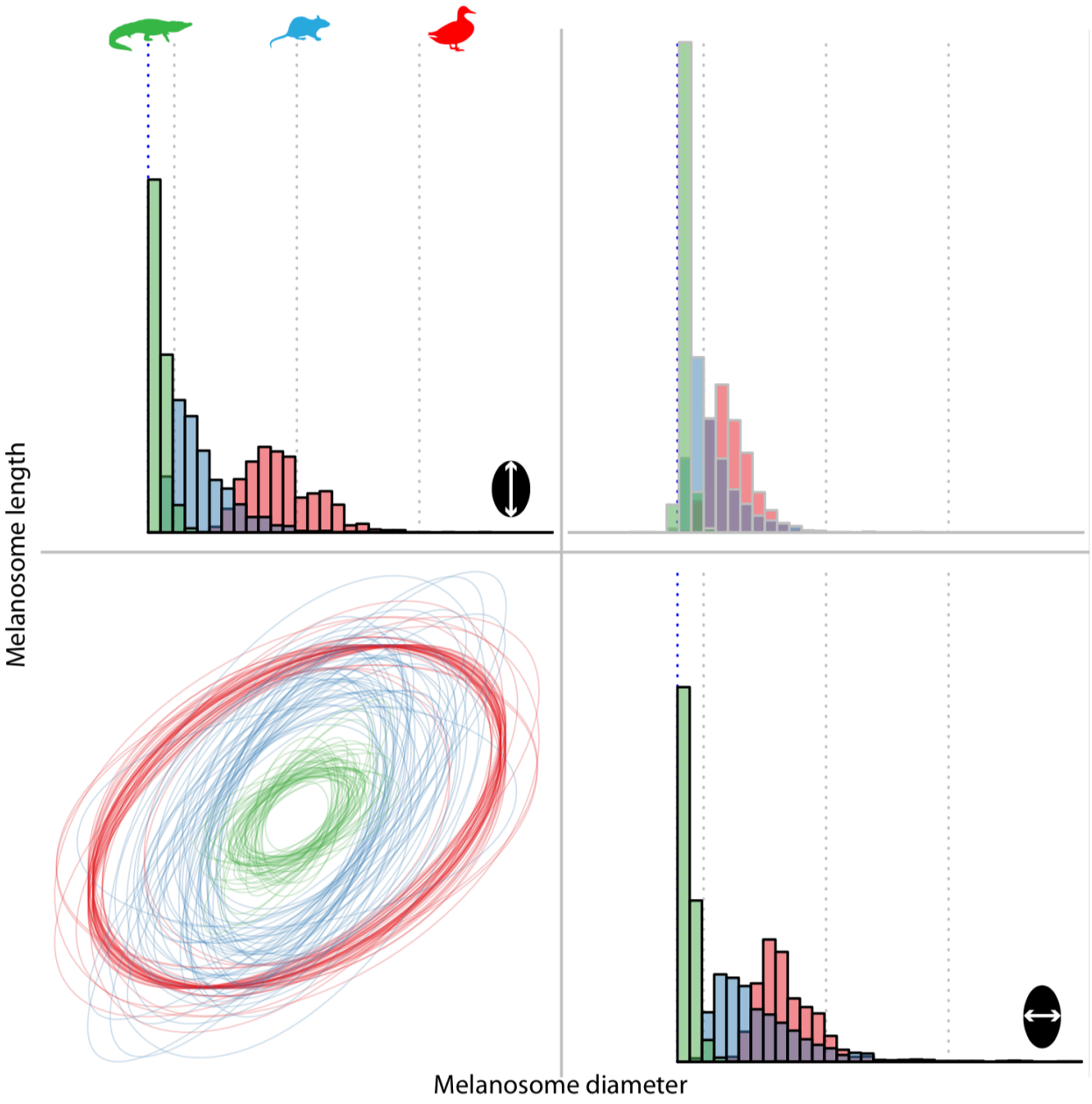

Figure S5. Weak among-clade differences in rates of melanosome shape evolution for brown (phaeomelanin-consistent) integument colours. Plots show evolutionary rates (diagonals) and covariance (off-diagonals) between melanosome length and diameter for birds (red), mammals (blue), and non-avian reptiles (green).

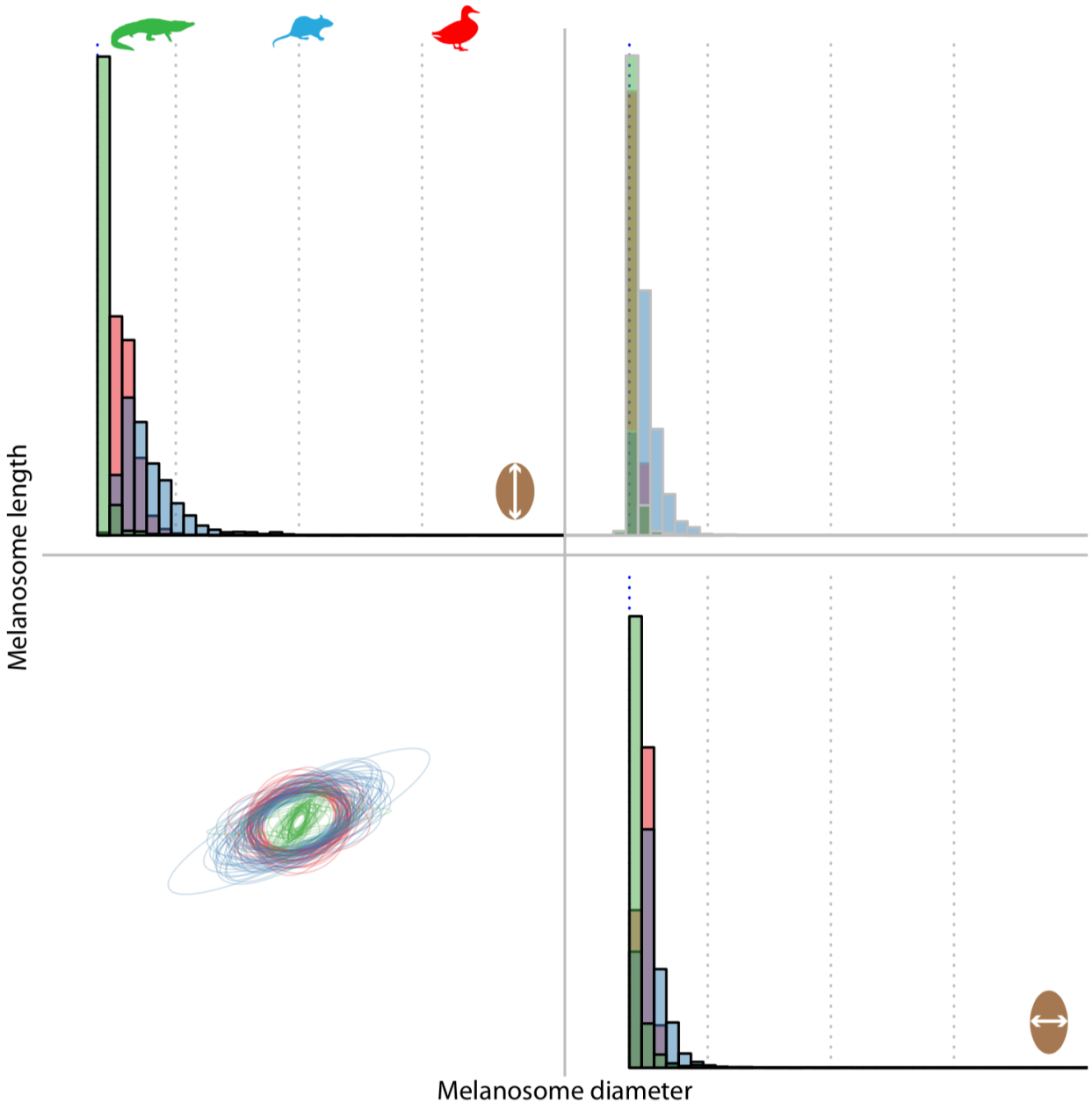

Figure S6. Relationship between melanosome morphology and resting metabolic rate. Results are for a subset of 31 species with both brown and black colour patches on the body.

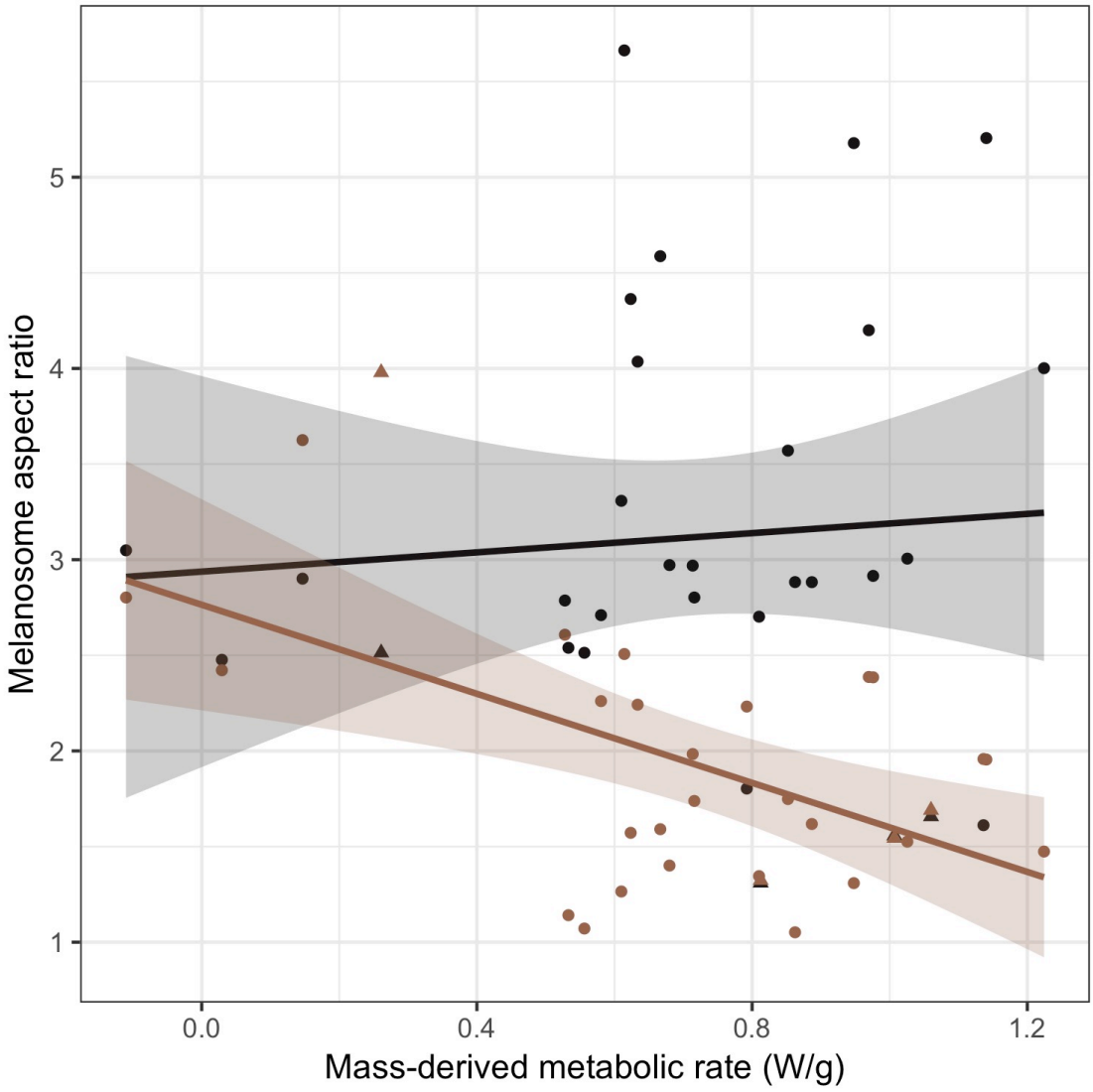

Figure S7. Relationship between melanosome morphology and mass-derived metabolic rate. Results are shown for a subset of 77 species with both body mass and mass-specific metabolic rate data. Slopes for best-fit lines are derived from MCMCglmm analyses.

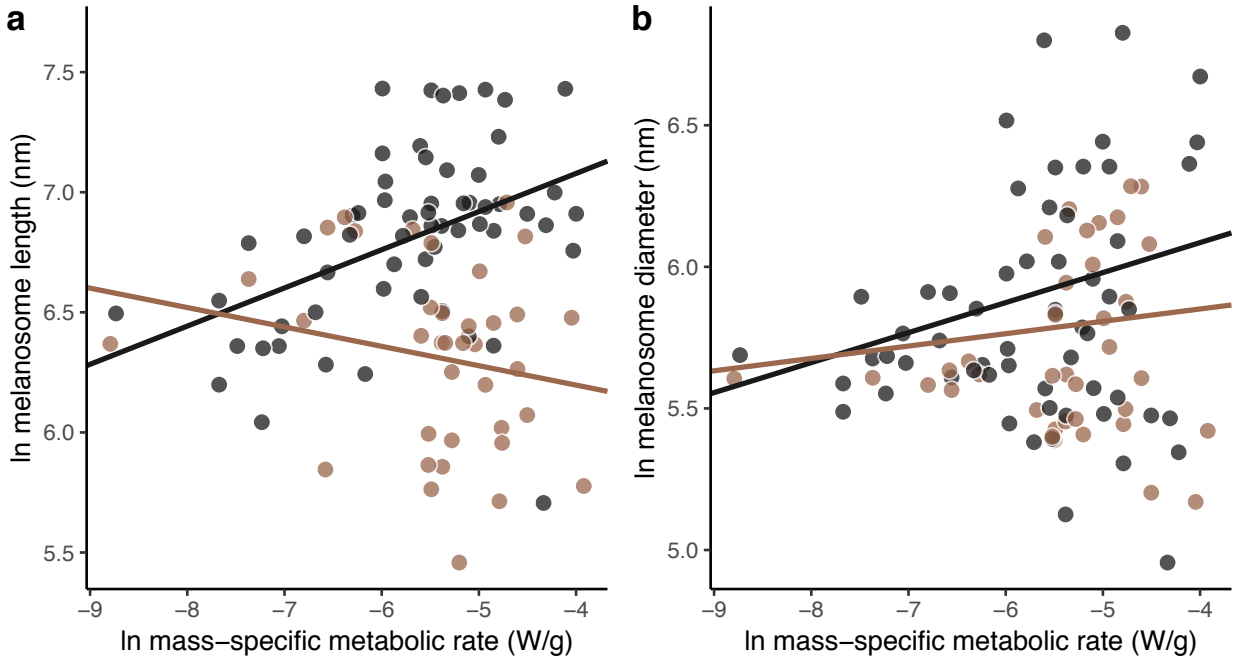

SUPPLEMENTARY REFERENCES

1. Webb C. 2000 Exploring the phylogenetic structure of ecological communities: an example for rain forest trees. *Am. Nat.* 156, 145–155.

2. Li Q, Clarke JA, Gao K-Q, Zhou C-F, Meng Q, Li D, D'Alba L, Shawkey MD. 2014 Melanosome evolution indicates a key physiological shift within feathered dinosaurs. *Nature* **507**, 350–353. (doi:10.1038/nature12973)

3. Benson RBJ, Campione NE, Carrano MT, Mannion PD, Sullivan C, Upchurch P, Evans DC. 2014 Rates of dinosaur body mass evolution indicate 170 million years of sustained ecological innovation on the avian stem lineage. *PLoS Biol.* 12, e1001853. (doi:10.1371/journal.pbio.1001853.s011)

4. Bapst DW. 2012 paleotree: an R package for paleontological and phylogenetic analyses of evolution. *Methods Ecol. Evol.* 3, 803–807. (doi:10.1111/j.2041-210X.2012.00223.x)

5. Clarke J. 2013 Feathers before flight. *Science* 340, 690–692. (doi:10.1126/science.1235463)

6. Ackerly D. 2000 Taxon sampling, correlated evolution, and independent contrasts. *Evolution* 54.

7. Close RA, Friedman M, Lloyd GT, Benson RBJ. 2015 Evidence for a mid-Jurassic adaptive radiation in mammals. *Curr. Biol.* 25, 2137–2142. (doi:10.1016/j.cub.2015.06.047)

8. Caetano Daniel S., Harmon Luke J. 2017 ratematrix: An R package for studying evolutionary integration among several traits on phylogenetic trees. *Methods Ecol. Evol.* 8, 1920–1927. (doi:10.1111/2041-210X.12826)

9. Huelsenbeck JP, Nielsen R, Bollback JP. 2003 Stochastic mapping of morphological characters. *Syst. Biol.* 52, 131–158. (doi:10.2307/3651122)

10. Eliason CM, Hudson L, Watts T, Garza H, Clarke JA. 2017 Exceptional preservation and the fossil record of tetrapod integument. *Proc. R. Soc. Lond. Ser. B-Biol. Sci.* 284, 20170556. (doi:10.1016/0031-0182(88)90096-X)

11. McNamara ME, Orr PJ, Kearns SL, Alcalá L, Anadón P, Mollá EP. 2009 Soft-tissue preservation in Miocene frogs from Libros, Spain: insights into the genesis of decay microenvironments. *Palaios* **24**, 104–117.

12. Plummer M, Best N, Cowles K, Vines K. 2006 CODA: convergence diagnosis and output analysis for MCMC. *R News* **6**, 7–11.

13. Li Q, Gao K-Q, Vinther J, Shawkey MD, Clarke JA, D'Alba L, Meng Q, Briggs DEG, Prum RO. 2010 Plumage color patterns of an extinct dinosaur. *Science* **327**, 1369–1372. (doi:10.1126/science.1186290)